Hindawi
Journal of Spectroscopy
Volume 2017, Article ID 5634384, 8 pages
https://doi.org/10.1155/2017/5634384

Research Article

Multiple Gamma-Ray Detection Capability of a $CeBr_3$ Detector for Gamma Spectroscopy

A. A. Naqvi,[1] F. Z. Khiari,[1] F. A. Liadi,[1] Khateeb ur-Rehman,[1] M. Raashid,[1] and A. A. Isab[2]

[1]*Department of Physics, King Fahd University of Petroleum and Minerals, Dhahran, Saudi Arabia*
[2]*Department of Chemistry, King Fahd University of Petroleum and Minerals, Dhahran, Saudi Arabia*

Correspondence should be addressed to A. A. Naqvi; aanaqvi@kfupm.edu.sa

Received 8 June 2017; Accepted 20 September 2017; Published 21 December 2017

Academic Editor: Javier Garcia-Guinea

The newly developed cerium tribromide ($CeBr_3$) detector has reduced intrinsic gamma-ray activity with gamma energy restricted to 1400–2200 keV energy range. This narrower region of background gamma rays allows the $CeBr_3$ detector to detect more than one gamma ray to analyze the gamma-ray spectrum. Use of multiple gamma-ray intensities in elemental analysis instead of a single one improves the accuracy of the estimated results. Multigamma-ray detection capability of a cylindrical 75 mm × 75 mm (diameter × height) $CeBr_3$ detector has been tested by analyzing the chlorine concentration in water samples using eight chlorine prompt gamma rays over 517 to 8578 keV energies utilizing a D-D portable neutron generator-based PGNAA setup and measuring the corresponding minimum detection limit (MDC) of chlorine. The measured MDC of chlorine for gamma rays with 517–8578 keV energies varies from 0.07 ± 0.02 wt% to 0.80 ± 0.24. The best value of MDC was measured to be 0.07 ± 0.02 wt% for 788 keV gamma rays. The experimental results are in good agreement with Monte Carlo calculations. The study has shown excellent detection capabilities of the $CeBr_3$ detector for eight prompt gamma rays over 517–8578 keV energy range without significant background interference.

1. Introduction

Gamma-ray spectroscopy techniques are continuously progressing due to rapid advances in the development and fabrication of fast and higher light output scintillation materials [1–3]. The development of the cerium tribromide ($CeBr_3$) gamma-ray detector among the lanthanum halide detector series ($LaBr_3$:Ce and $LaCl_3$:Ce detectors) is one such example [4–11]. The $CeBr_3$ detector, which has an energy resolution comparable with that of a $LaCl_3$:Ce detector, has an order of magnitude reduced intrinsic activity as compared to the $LaBr_3$:Ce and $LaCl_3$:Ce detector [9]. Furthermore, the reduced intrinsic activity of the CeBr3 detector has a narrower energy range of 1400–2200 keV [9, 12], as compared to 780–2200 keV energy range reported for the intrinsic activity of the $LaBr_3$:Ce and $LaCl_3$:Ce ([1, 3, 7]). These features enable the $CeBr_3$ detector to provide a larger interference-free energy range for the gamma-ray detection in prompt gamma-ray analysis of bulk samples as compared to the $LaBr_3$:Ce and $LaCl_3$:Ce detectors.

In the present study, the multiple gamma-ray detection capabilities of a cylindrical 76 mm × 76 mm (diameter × height) $CeBr_3$ detector were studied through chlorine concentration measurements in saline water samples utilizing eight chlorine prompt gamma rays [13] in conjunction with a portable neutron generator-based PGNAA setup [8, 12]. The saline water samples were chosen due to their significance as secondary calibration standards. The prompt gammas emitted from chlorine are considered as secondary standards for detector calibrations because of the high-thermal neutron capture cross section of chlorine and also because of the wide range of high-intensity gamma emissions up to 8.5 MeV [14].

Furthermore, the chlorine analysis in saline water samples is also very important for the assessment of groundwater and surface water pollution program of the Environmental

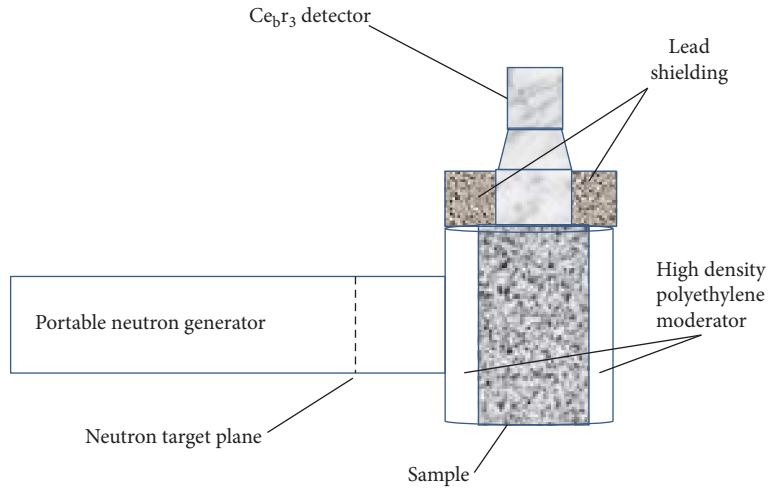

Figure 1: Schematic representation of the MP320 portable neutron generator-based PGNAA setup used to measure the prompt gamma-ray yields.

Studies [15, 16]. Chloride in water has adverse effects on the environment and industry. The U.S. Environmental Protection Agency (USEPA) has imposed an upper limit of 250 mg/L for maximum contaminant level (SMCL) of chloride in drinking water [16].

In the present study, the multiple gamma-ray detection capabilities of a cylindrical 76 mm × 76 mm (height × diameter) Ce:Br_3 detector has been tested through analysis of saline water samples containing 0.0–8.0 wt% chlorine concentrations. The experimental data was acquired for eight chlorine prompt gamma rays and minimum detectable concentration (MDC) for each gamma-ray line was estimated. For comparison, the intensities of chlorine prompt gamma rays from the saline water samples were also calculated using the MCNP4B2 code [17].

For comparison with the $CeBr_3$ detector, the prompt gamma-ray spectrum from a cylindrical 76 mm × 76 mm (diameter × height) $LaCl_3$:Ce detector was acquired with the saline water samples. Details of this study are reported in the following sections of the paper.

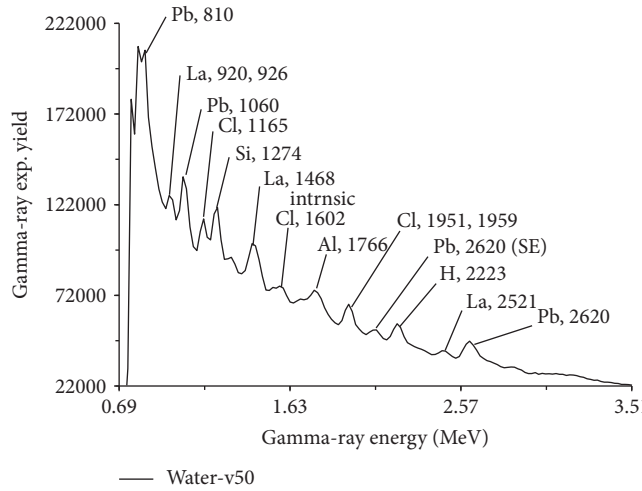

Figure 2: Prompt gamma-ray spectrum due to activation of the LaCl3:Ce detector caused by the capture of thermal neutrons in La, Ce and Cl in LaCl3:Ce detector material over 0.69–3.51 MeV range.

2. Prompt Gamma Spectrum of $LaCl_3$:Ce Detector with Water Sample

The prompt gamma-ray spectrum from a $LaCl_3$:Ce detector was measured using the portable neutron generator-based PGNAA set up described earlier [8] and shown in Figure 1. It will be described briefly. The setup contains a high-density polyethylene cylindrical moderator with a concentric central cylindrical cavity for a cylindrical sample container with 106 mm × 1.5 mm (diameter × length). Moreover, a cylindrical 76 mm × 76 mm (diameter × length) $LaCl_3$:Ce or $CeBr_3$ gamma-ray detector views the sample through the cavity hole at a right angle to the neutron generator axis. The empty polyethylene plastic sample container has a mass of 96 g and a density of 0.92 g/cm^3. The paraffin and lithium carbonate mixed neutron shield is used to protect the detector against neutrons while lead shielding provides detector protection against gamma rays. For the tests of the $LaCl_3$:Ce detector, the plastic sample bottle was filled with pure water.

MeV neutrons were produced using the D(d,n) reaction using a 70 μA pulsed deuteron beam of 70 keV energy, a width of 800 microseconds and a frequency of 250 Hz. The prompt gamma-ray spectrum of the $LaCl_3$:Ce detector from the pure water samples was counted for 25 min. The neutron flux was monitored using a beam current monitor from the neutron generator. Any fluctuation in the beam current was taken into account while normalizing the data.

Figures 2 and 3 show the gamma-ray spectra of the $LaCl_3$:Ce detector for the water sample. Figure 2 shows the gamma-ray background spectrum over 0.69–3.51 MeV energy range. The spectrum shows background gamma-ray peaks from detector material as well as shielding material used in the PGNAA setup. Noticeable capture peaks from

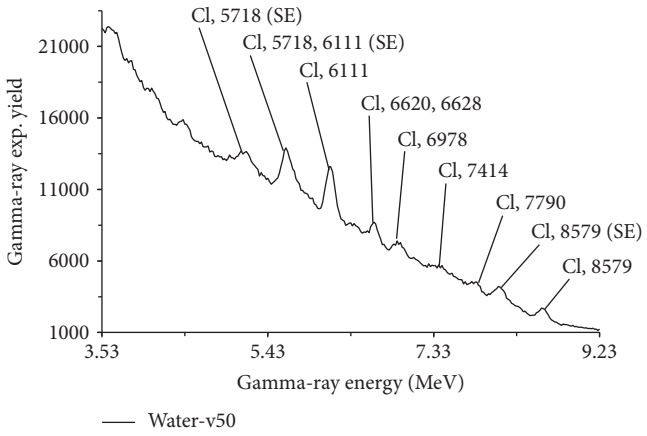

Figure 3: Prompt gamma-ray spectrum due to activation of the LaCl3:Ce detector caused by the capture of thermal neutrons in La, Ce, and Cl in LaCl3:Ce detector material over 3.53–9.23 MeV range.

detector material are La(920), La(926), and La(2521) peaks along with La(1468) intrinsic peak. Also shown are capture peaks Cl(1165), Cl(1602), and Cl(1951, 1959) due to chlorine in the detector, along with Pb(810), Pb(1060) and Pb(2620) peaks from shielding material. Also, Si(1274) and Al(1766) prompt gamma rays are shown along with hydrogen H(2223) capture peak.

Figure 3 shows the background gamma-ray spectrum from the water sample over 3.53–9.23 MeV energy range taken with the $LaCl_3$:Ce detector. Noticeable capture peaks from chlorine in the detector material are Cl(5718), Cl(6111), Cl(6620, 6628), Cl(6978), Cl(7414), Cl(7790), and C(8579).

This study has shown that multiple energy chlorine background gamma-ray peaks from $LaCl_3$:Ce makes its use in the detection of chlorine quite difficult and inaccurate. A $CeBr_3$ detector can be a good substitute for the $LaCl_3$:Ce detector in the chlorine measurements and this study was undertaken to verify this fact.

3. Prompt Gamma-Ray Intensity Calculations from Saline Water Samples

Prior to the gamma-ray measurements with a $CeBr_3$ detector, the intensities of chlorine prompt gamma rays from water samples were calculated using the general purpose MCNP4B2 code [17]. The intensities of eight chlorine gamma rays, namely, 517, 788, 1165, 1951, 2863, 6110, 6619, and 8578 keV were calculated for saline water samples containing 0.0–8.0 wt% chlorine. The calculations were carried out for the 2.5 MeV neutron-based PGNAA setup using the procedure described earlier [8]. For calculation, the sample was divided into subcells of 1 cm thickness, which allowed the transport of the neutrons and gamma rays of appropriate statistical weight to the next adjacent cell, without any loss. The F4 tally was used to calculate gamma-ray intensity in the detector volume. Saline water samples were prepared by thoroughly mixing water with 0.0–8.0 wt% chlorine. Gamma-ray yields were calculated for 517, 788, 1165, 1951,

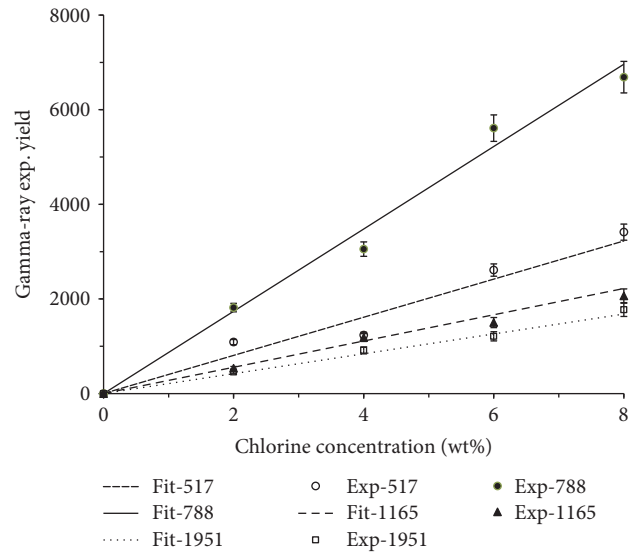

Figure 4: Integrated yield of 517, 788, 1165, and 1951 keV prompt gamma-ray spectra of the $CeBr_3$ detector from chlorine contaminated water samples plotted as a function of chlorine concentration. The lines show normalized-calculated yields of the gamma rays obtained through Monte Carlo calculations.

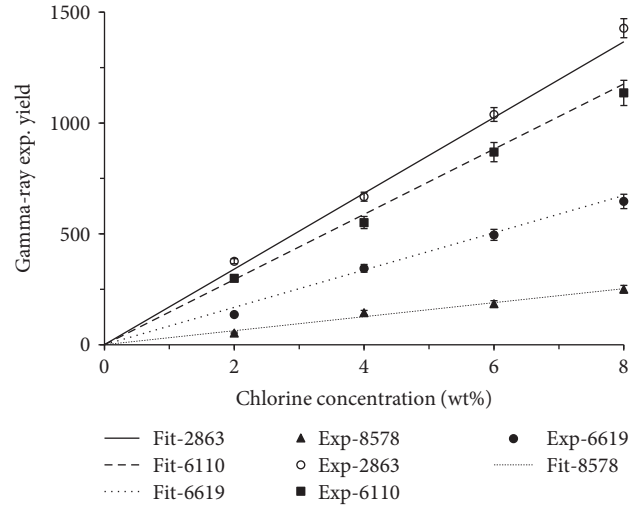

Figure 5: Integrated yield of 2863, 6110, 6619, and 8578 keV prompt gamma-ray spectra of the $CeBr_3$ detector from chlorine-contaminated water samples plotted as a function of chlorine concentration. The lines show normalized-calculated yields of the gamma rays obtained through Monte Carlo calculations.

2863, 6110, 6619, and 8578 keV chlorine prompt gamma rays produced due to capture of thermal neutrons in chlorine. Thermal neutrons were produced through moderation of 2.5 MeV neutrons in the moderator as well as in the water samples.

The calculated intensities of 517, 788, 1165, 1951, 2863, 6110, 6619, 8578 keV gamma rays increase with chlorine concentration but each line has a different slope. Among the low energy 517, 788, 1165, and 1951 keV chlorine gamma rays, the 788 keV line has maximum slope while for the

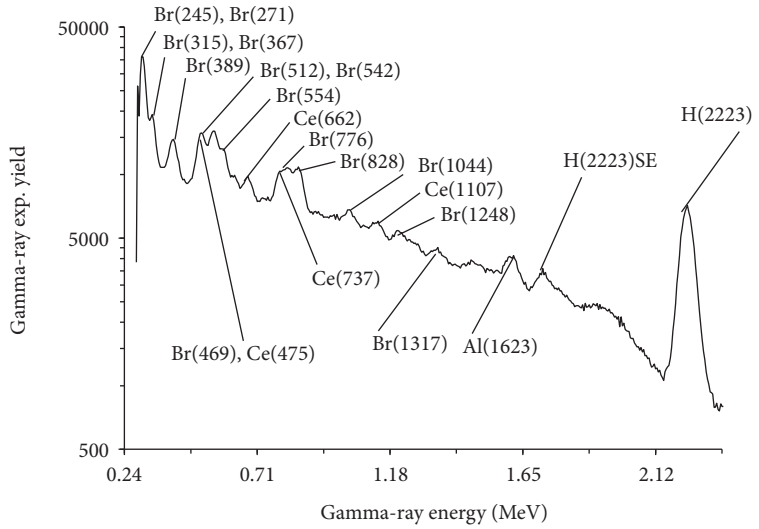

Figure 6: Prompt gamma-ray spectrum due to activation of the $CeBr_3$ detector caused by the capture of thermal neutrons in Br and Ce elements present in the $CeBr_3$ detector along with hydrogen capture peak from the moderator.

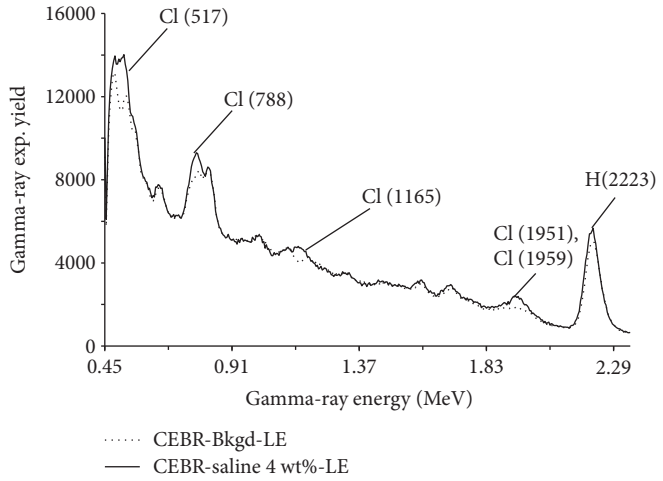

Figure 7: Low-energy pulse height spectrum of the $CeBr_3$ detector for a saline water sample over 0.45–2.29 MeV range from a 4% chlorine-contaminated water sample superimposed upon background spectrum.

high energy 2863, 6110, 6619, and 8578 keV chlorine gamma rays, the maximum slope has been observed for the 2863 keV gamma rays. The calculated yield curves of 517, 788, 1165, 1951, 2863, 6110, 6619, and 8578 keV prompt gamma rays are plotted along with the experimental data in Figures 4 and 5.

4. Prompt Gamma Measurements Using the $Cebr_3$ Detector

Prompt gamma-ray measurements from saline water samples were carried out using the $CeBr_3$ detector in conjunction with the portable neutron generator and following the procedure given in Section 2.

Prompt gamma rays from chlorine have several intense lines with energies varying from 0.5 MeV to 8.6 MeV. In order to obtain optimum resolution of these gamma rays, the measurements were carried out with two different pulse height amplifier gain settings. One amplifier setting, with larger gain, was used to acquire gamma-ray pulse height spectrum over 0.00–2.22 MeV while the other amplifier setting, with smaller gain, was used to acquire gamma-ray pulse height spectrum over 1.45–9.98 MeV.

The larger gain setting of the amplifier was used to record low energy gamma rays with energies below 2.22 MeV by adjusting the hydrogen peak location near the end channel of the spectrum, as shown in Figure 6 which shows the low energy activation spectrum of the $CeBr_3$ detector due to the capture of thermal neutrons in the $CeBr_3$ detector material. The prompt gamma peaks due to the capture of thermal neutrons in Ce, Br, and H (from moderator material) are quite prominent. Figure 7 shows the low energy prompt gamma-

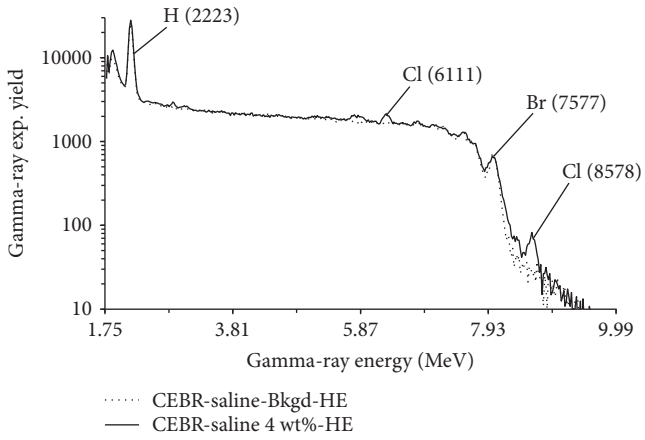

Figure 8: High-energy pulse height spectrum of the $CeBr_3$ detector for a saline water sample over 1.75–9.98 MeV range from a 4% chlorine-contaminated water sample superimposed upon background spectrum.

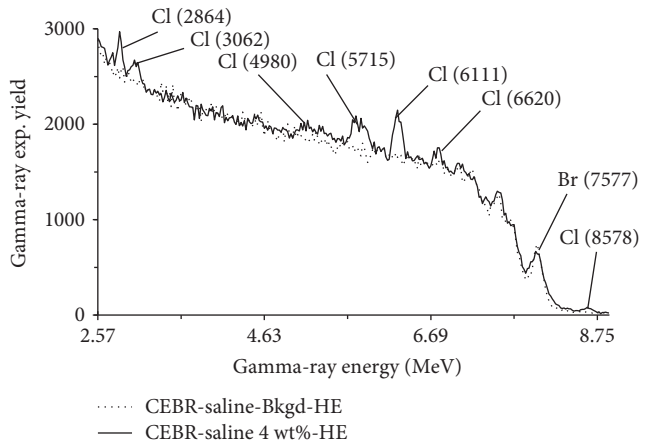

Figure 9: Enlarged high-energy pulse height spectrum of the $CeBr_3$ detector for a saline water sample over 2.57–8.75 MeV range from a 4% chlorine-contaminated water sample superimposed upon background spectrum.

ray spectrum from saline water samples containing 4.0 wt% chlorine superimposed upon the background spectrum over 0.41–2.29 MeV energy range. Chlorine peaks at 517, 788, 1165, and 1951–1959 keV along with the 2223 keV hydrogen peak from the moderator are quite prominent.

The smaller gain setting of the amplifier was used to record high energy gamma rays with 1.45–9.98 MeV energies by adjusting the location of the hydrogen peak near the beginning channels of the spectrum, as shown in Figure 8 which shows the high energy prompt gamma-ray spectrum from saline water samples containing 4 wt% chlorine along with the background spectrum over 1.75–9.98 MeV energy range. Chlorine peaks at 6111 and 8578 keV along with the 2223 keV hydrogen peak are quite prominent. Figure 9 shows the enlarged part of Figure 8 over 2.57–8.75 MeV range showing 2864, 3062, 4980, 5715, 6111, 6620, and 8578 keV chlorine peaks.

Table 1: Energies and partial elemental cross section $\sigma_\gamma{}^z(E_\gamma)$ barns of prominent capture gamma rays of bromine, cerium, and chlorine [13].

Element	Gamma-ray energy (keV)	$\sigma_\gamma{}^z(E_\gamma)$ barns
Br	196	0.43
	271	0.46
	275	0.16
	315	0.46
	367	0.23
	513	0.21
	661	0.08
	828	0.28
	1248	0.053
	7577	0.10
Ce	475	0.082
	662	0.241
	1107	0.040
Ni	8533	0.721
	8998	1.49
Cl	517	7.58
	786	3.42
	788	5.42
	1165	8.91
	1601	1.21
	1951	6.33
	1959	4.10
	2864	1.82
	3062	1.13
	4980	1.23
	5715	1.82
	6111	6.59
	6619	2.53
	7414	3.29
	7790	2.66
	8578	0.88

In order to calibrate the detector for the higher energy gamma rays, the detector spectrum was acquired from a $NiNO_3$ sample and the spectrum was calibrated using high energy Ni (8533) and Ni(8998) keV gamma rays along with the Br(7577) gamma-ray peak from the detector material.

For each amplifier setting, the detector background spectrum was recorded with an empty plastic container inserted into the moderator cavity. The background spectrum of the $CeBr_3$ detector contains capture gamma-ray peaks of Br and Ce elements present in the $CeBr_3$ detector material. The energies and intensities of prominent capture prompt gamma ray in cerium and bromine are listed in Table 1 [13]. The background spectrum is subtracted from the sample spectrum to obtain the difference gamma-ray spectrum of the sample. The prompt gamma-ray data from the chloride-contaminated water samples were acquired for a

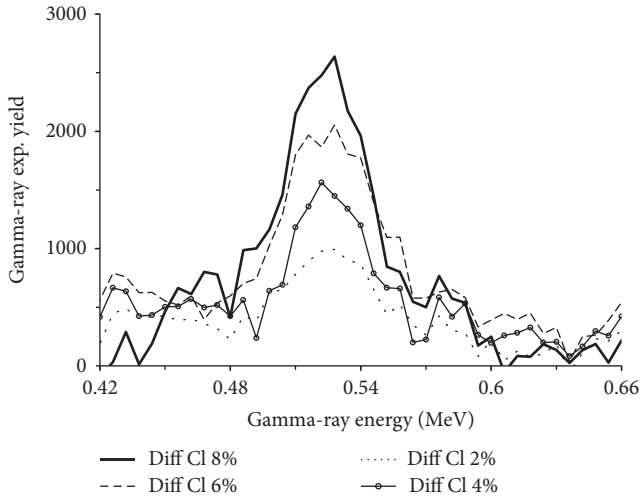

Figure 10: Pulse height difference spectra of the $CeBr_3$ detector for 517 keV chlorine gamma rays from 2%, 4%, 6%, and 8% chlorine-contaminated water samples over 0.42–0.66 MeV range superimposed upon each other.

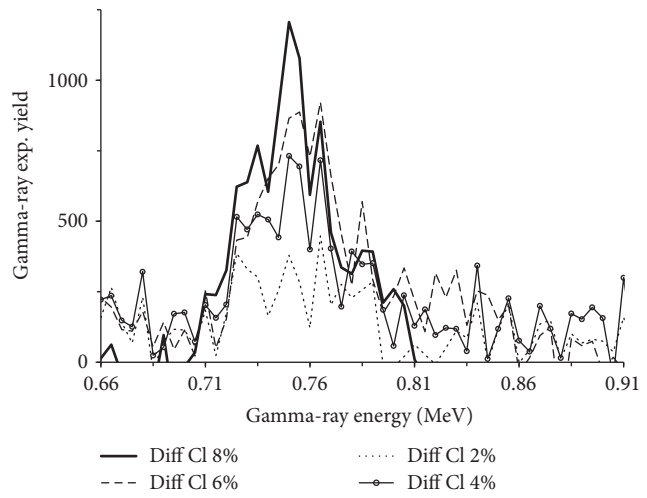

Figure 11: Pulse height difference spectra of the $CeBr_3$ detector for 776–778 keV chlorine gamma rays from 2%, 4%, 6%, and 8% chlorine-contaminated water samples over 0.66–0.91 MeV range superimposed upon each other.

preset time of 20–30 min. Low and high energy gamma-ray spectra from saline water samples containing 2, 4, 6, and 8 wt% chlorine were analyzed using pulse height windows corresponding to 517, 788, 1165, 1951, 2863, 6110, 6619, and 8578 keV chlorine prompt gamma rays.

5. Results and Discussion

For each gamma ray, the energy difference spectrum was generated for 2%, 4%, 6%, and 8% chlorine by subtracting the background spectrum from the sample spectrum and normalizing to the same neutron flux. Finally, the area under each difference peak was integrated to generate the gamma yield as a function of chlorine concentration. Then, the gamma-ray yield versus concentration curve was plotted. This process was repeated for each of the eight chlorine gamma rays with 517, 786–788, 1165, 1951–1959, 2863, 6110, 6620, and 8578 keV and eight difference spectra were analyzed. In the following, only three representative gamma-ray difference spectra are shown for which we obtained the best value of MDC.

Figures 10, 11, and 12 show gamma-ray difference spectra of 517, 786–788 keV, and 1951–1959 keV gamma rays. For these three gamma rays, we have found the best values of MDC for chlorine detection in water samples. Figure 10 shows the 517 keV peak over 0.42–0.66 MeV energy range while Figure 11 shows 786–788 keV chlorine peak over 0.66–0.91 MeV energy range. Figure 12 shows the 1951–1959 keV chlorine peak over 1.78–2.13 MeV energy range.

The integrated gamma ray yields of chlorine for the eight gamma rays as a function of chlorine concentration in the saline water samples are shown in Figures 4 and 5 where the experimental data points for each gamma ray are superimposed on the Monte Carlo calculated yield of the respective gamma ray. The experimental results are in agreement with the calculated values.

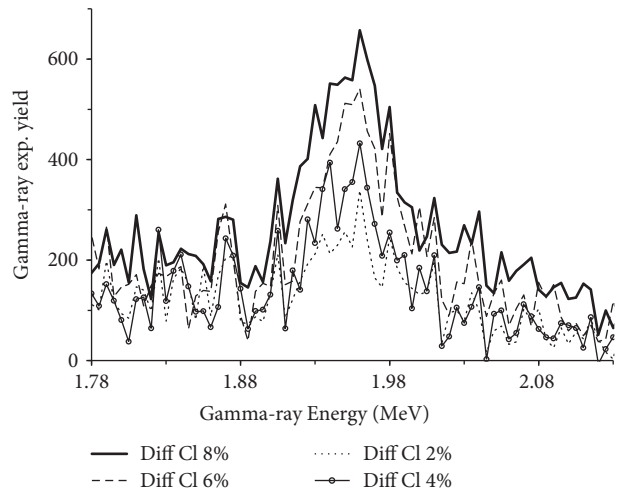

Figure 12: Pulse height difference spectra of the $CeBr_3$ detector for 1951–1959 keV chlorine gamma rays from 2%, 4%, 6%, and 8% chlorine-contaminated water samples over 1.78–2.13 MeV range superimposed upon each other.

Figure 4 shows the integrated yield of 517, 788, 1165, and 1951 keV gamma rays as a function of chlorine concentration. Among this group of chlorine gamma-ray lines, the maximum slope has been observed for 788 keV gamma rays while the minimum slope was for 1951 keV gamma rays. Figure 5 shows the integrated yield of 2863, 6110, 6619, and 8578 keV chlorine gamma for various chlorine concentrations. Among this group of chlorine gamma-ray lines, the maximum slope has been observed for 2863 keV gamma rays while the minimum slope has been observed for 6619 keV gamma rays.

5.1. Minimum Detection Limits for 0.5–8.58 MeV Chlorine Gamma Rays. The minimum detectable concentrations (MDCs) of the $CeBr_3$ detector-based PGNAA setup were

Table 2: Minimum detectable concentration (MDC) of chlorine in water samples for various gamma rays using $CeBr_3$ detector along with portable neutron generator-based PGNAA setup.

Cl-gamma ray energy (keV)	$CeBr_3$ detector	
	MDC (wt%)	σ_{MDC} (wt%)
517	0.08	0.02
786–788	0.07	0.02
1165	0.18	0.05
1951/1959	0.11	0.03
2863	0.17	0.05
6111	0.13	0.04
6619	0.18	0.05
8578	0.80	0.24

determined for 517, 786–788, 1165, 1951–1959, 2863, 6111, 6619, and 8578 keV Cl gamma rays using the method published earlier [8]. Due to the limited neutron flux from the 2.5 MeV portable neutron generator, all MDCs are in the wt% range. For our cylindrical water samples, the MDCs for the eight chlorine prompt gamma rays vary from 0.07 wt% to 0.80 wt%. The values (MDCs) for each gamma ray along with its standard deviation σ_{MDC} are listed in Table 2.

Most of the MDC values vary over 0.07 ± 0.02 wt% to 0.18 ± 0.05 wt% with an exceptionally large value of MDC of 0.80 ± 0.24 for 8578 keV gamma. The larger MDCs have been obtained for the less intense peaks and/or peaks having a higher background underneath due to gamma rays produced from the $CeBr_3$ detector material. The smaller MDCs have been obtained for those gamma rays with higher intensities and relatively smaller background under the gamma-ray peak.

The optimum value of MDCs $\pm \sigma_{MDC}$ (wt%) was measured to be 0.07 ± 0.02 wt% and 0.08 ± 0.02 wt% for 517 keV and 786–788 keV chlorine gamma rays, respectively.

Although the1165 keV gamma rays have a large production cross section, yet a larger value of 0.18 ± 0.05 wt% of MDC has been measured for this gamma ray. This is due to the 1165 keV chlorine gamma-ray interference with of Ce(1107) gamma rays from the $CeBr_3$ detector material.

The 1951–1959 keV and 6111 keV gamma rays have large production cross sections but, within statistical uncertainty, they have equal MDCs, that is, 0.11 ± 0.03 wt% and 0.13 ± 0.04 wt%, respectively. For the remaining gamma rays, the measured MDCs are larger because they have smaller production cross sections. This study has shown the excellent multiple gamma-ray detection capabilities of the $CeBr_3$ detector for gamma-ray spectroscopy.

6. Conclusion

In this study, suitability of $LaCl_3$:Ce and $CeBr_3$ detectors for chlorine measurements was studied by comparing neutron beam-associated gamma-ray background of $LaCl_3$:Ce and $CeBr_3$ detectors. The comparison revealed very low gamma-ray background for the $CeBr_3$ detector while for the $LaCl_3$:Ce detector background showed additional chlorine thermal neutron for Cl(1165), Cl(1602), Cl(1951, 1959), Cl(5718), Cl(6111), Cl(6620, 6628), Cl(6978), Cl(7414), Cl(7790), and C(8579) gamma rays. This made the $LaCl_3$:Ce detector not suitable for chlorine measurements while $CeBr_3$ could be a good substitute of $LaCl_3$:Ce detector for chlorine measurements in bulk sample.

Then multigamma-ray detection capability of a cylindrical 75 mm × 75 mm (diameter × height) $CeBr_3$ detector has been tested by analyzing the chlorine concentration in water samples using eight chlorine prompt gamma rays 517, 786–788, 1165, 1951–1959, 2863, 6111, 6619, and 8578 keV chlorine over 517 to 8578 keV energies utilizing a D-D portable neutron generator-based PGNAA setup and measuring the corresponding minimum detection limit (MDC) of chlorine.

The MDC values for these gamma rays have been determined to be 0.08 ± 0.02, 0.07 ± 0.02, 0.18 ± 0.05, 0.11 ± 0.03, 0.17 ± 0.05, 0.13 ± 0.04, 0.18 ± 0.05, 0.80 ± 0.24 wt%, respectively. The experimental results agree with Monte Carlo results. The best MDC values of 0.07 ± 0.02 and 0.08 ± 0.02 wt% have obtained for 786–788 and 517 keV gamma rays, respectively. The $CeBr_3$ detector has proven to be an excellent multiple gamma-ray detectors.

Conflicts of Interest

The authors declare that they have no conflicts of interest.

Acknowledgments

This study was carried out under NSTIP Project no. ENV2367-04 funded by KACST, Saudi Arabia. The authors gratefully acknowledge the support provided by the Physics Department, King Fahd University of Petroleum and Minerals, Dhahran, Saudi Arabia.

References

[1] D. Alexiev, L. Mo, D. A. Prokopovich, M. L. Smith, and M. Matuchova, "Comparison of $LaBr_3$: Ce and $LaCl_3$: Ce with NaI(Tl) and cadmium zinc telluride (CZT) detectors," *IEEE Transactions on Nuclear Science*, vol. 55, 2008, no. 3, pp. 1174–1177, 2008.

[2] N. J. Cherepy, S. A. Payne, S. J. Asztalos et al., "Scintillators with potential to supersede lanthanum bromide," *IEEE Transactions on Nuclear Science*, vol. 56, no. 3, pp. 873–880, 2010.

[3] P. R. Menge, G. Gautier, A. Iltis, C. Rozsa, and V. Solovyev, "Performance of large lanthanum bromide scintillators," *Nuclear Instruments and Methods in Physics Research Section A: Accelerators, Spectrometers, Detectors and Associated Equipment*, vol. 579, no. 1, pp. 6–10, 2007.

[4] P. Dorenbos, "Light output and energy resolution of Ce^{3+}-doped scintillators," *Nuclear Instruments and Methods in Physics Research Section A: Accelerators, Spectrometers, Detectors and Associated Equipment*, vol. 486, no. 1-2, pp. 208–213, 2002.

[5] W. Drozdowski, P. Dorenbos, A. J. Bos, G. Bizarri, A. Owens, and F. G. Quarati, "$CeBr_3$ scintillator development for possible use in space missions," *IEEE Transactions on Nuclear Science*, vol. 55, no. 3, pp. 1391–1396, 2008.

[6] P. Guss, M. Reed, D. Yuan et al., "Size effect on nuclear gamma-ray energy spectra acquired by different-sized $CeBr_3$, $LaBr_3$:Ce, and NaI:Tl gamma-ray detectors," *Nuclear Technology*, vol. 185, no. 3, pp. 309–321, 2014.

[7] P. Guss, M. Reed, D. Yuan, M. Cutler, C. Contreras, and D. Beller, "Comparison of $CeBr_3$ with $LaBr_3$:Ce, $LaCl_3$:Ce, and NaI:Tl detectors," in *Proceedings Volume 7805, Hard X-Ray, Gamma-Ray, and Neutron Detector Physics XII, 78050L*, 2010.

[8] A. A. Naqvi, F. Z. Khiari, F. A. Liadi, U.-R. Khateeb-, and A. A. Isab, "Performance tests of a large volume cerium tribromide ($CeBr_3$) scintillation detector," *Applied Radiation and Isotopes*, vol. 114, pp. 50–56, 2016.

[9] F. G. Quarati, P. Dorenbos, J. Van der Biezen et al., "Scintillation and detection characteristics of high-sensitivity $CeBr_3$ gamma-ray spectrometers," *Nuclear Instruments and Methods in Physics Research Section A: Accelerators, Spectrometers, Detectors and Associated Equipment*, vol. 729, pp. 596–604, 2013.

[10] F. G. Quarati, M. S. Alekhin, K. W. Krämer, and P. Dorenbos, "Co-doping of $CeBr_3$ scintillator detectors for energy resolution enhancement," *Nuclear Instruments and Methods in Physics Research Section A: Accelerators, Spectrometers, Detectors and Associated Equipment*, vol. 735, pp. 655–658, 2014.

[11] D. N. Ter Weele, D. R. Schaart, and P. Dorenbos, "The effect of self-absorption on the scintillation properties of Ce^{3+} activated $LaBr_3$ and $CeBr_3$," *IEEE Transactions on Nuclear Science*, vol. 61, no. 1, pp. 683–688, 2014.

[12] A. A. Naqvi, F. Z. Khiari, F. A. Liadi, U.-R. Khateeb-, and A. A. Isab, "Energy resolution measurements of $CeBr_3$ and $LaCl_3$:Ce detectors," *Journal of Radioanalytical and Nuclear Chemistry*, vol. 310, no. 2, pp. 849–855, 2016.

[13] H. D. Choi, R. B. Firestone, R. M. Lindstrom et al., *Database of Prompt Gamma-Rays from Slow Neutron Capture for Elemental Analysis*, INTERNATIONAL ATOMIC ENERGY AGENCY, Vienna, Austria, 2006.

[14] G. L. Molnár, Z. Révay, and T. Belgya, "Accurate absolute intensities for the ^{35}Cl (n,γ) reaction gamma-ray standard," *Nuclear Instruments and Methods in Physics Research Section B: Beam Interactions with Materials and Atoms*, vol. 213, pp. 32–35, 2004.

[15] J. R. Mullaney, D. L. Lorenz, and A. D. Arntson, "Chloride in groundwater and surface water in areas underlain by the glacial aquifer system, Northern United States," National Water-Quality Assessment Program Scientific Investigations Report # 2009–5086, U.S. Department of the Interior and U.S. Geological Survey, 2009, http://www.usgs.gov.

[16] U.S. Environmental Protection Agency, *Secondary Drinking Water Regulations—Guidance for Nuisance Chemicals: EPA 810/K–92–001*, 1992, http://www.epa.gov/safewater/consumer/2ndstandards.html.

[17] J. F. Briesmeister, Ed., "MCNP4B2 –a General Monte Carlo N-particles transport code," Los Alamos National Laboratory Report, LA-12625. Version 4C, Los Alamos National Laboratory Report, LA-12625-M, 1997.